

Short Communication

## Label-free Electrochemical Sensor for MicroRNA Detection based on a Gold Nanoparticles@Poly(methylene blue)-Modified Electrode and a Target Cyclic Amplification Strategy

Weiwei Wang

Institution of Biology and Food Engineering, Suzhou University, Suzhou 234000, China

E-mail: [249432388@qq.com](mailto:249432388@qq.com)

Received: 30 December 2019 / Accepted: 22 February 2020 / Published: 10 April 2020

---

Herein, a gold nanoparticles (AuNPs)/poly(methylene blue) (PMB)-modified electrode was fabricated and employed to sensitively detect microRNA (miRNA). A PMB film was electropolymerized onto the surface of a glass carbon electrode (GCE). AuNPs were immobilized onto the PMB/GCE surface, which provided a platform for the immobilization of probe DNA (pDNA) via Au-S bonds. In our strategy, when target miRNA was present, a target cyclic amplification reaction was triggered, which resulted in an electrochemical behaviour change at the PMB-solution interface. The signal change, which resulted from DNA hybridization generated on the electrode surface, was used to detect target miRNA with differential pulse voltammetry (DPV). The experimental results showed that the proposed sensor could detect miRNA-21 with high sensitivity and selectivity. The DPV peak current change ( $\Delta I$ ) showed a good linear relationship with the logarithm of concentration in a range of  $1.0 \times 10^{-13}$  -  $1.0 \times 10^{-9}$  mol/L, and the detection limit was  $3.0 \times 10^{-14}$  mol/L ( $S/N=3$ ). In addition, the sensor had good stability and reproducibility. Thus, the as-produced sensor has good application prospects in miRNA analysis.

---

**Keywords:** Gold nanoparticles; Poly(methylene blue); MicroRNA; Electrochemical sensor; Differential pulse voltammetry

### 1. INTRODUCTION

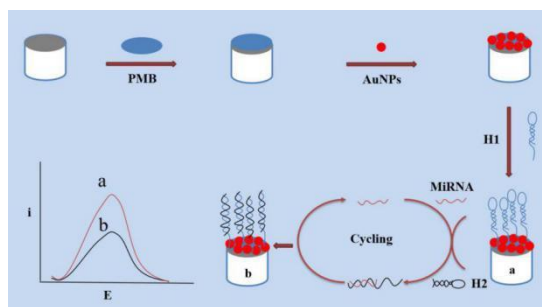
MicroRNA (miRNA) is a kind of single-stranded small molecule with a length of approximately 18-24 nucleotides [1], which is the smallest functional non-coding RNA that widely exists in animals, plants, viruses and other organisms [2]. The biological function of miRNA is a hot spot that researchers pay considerable attention to. The abnormal expression of miRNAs is related to various diseases, such as cancers[3]. To study biological functions of miRNAs, the development of a highly sensitive detection method is key. Recently, the detection methods of miRNA mainly include northern blotting[4], fluorescence[5-8], microarray analysis[9-10] and electrochemistry[11-15]. Among these methods, label-

free electrochemical miRNA sensors have been widely studied because of their advantages, which include their fast response, high sensitivity and selectivity, low cost, and easy micro-miniaturization.

Methylene blue (MB), a cationic dye of the phenothiazine type, is a kind of active electron transfer molecule[16]. Previous reports have indicated that MB can aggregate after a pretreatment of the electrode surface into a layer of conductive polymer film, which has good electrochemical activity and electrical catalytic properties. Electropolymerization of MB on the electrode surface can not only increase the adsorption strength but also accelerate the charge transfer rate. Recently, PMB-based electrochemical sensors have been developed and applied to assay biomolecules [17,18]. Gold nanoparticles (AuNPs) have dielectric properties and demonstrate catalytic action; furthermore, they can bind to a variety of biological macromolecules without affecting their biological activity. Importantly, because of its surface plasma and special biocompatibility, it can bind with other probes (such as DNA probes) via an Au-S bond. AuNP-based electrochemical sensors have been designed and applied in miRNA assays [19, 20].

Target cyclic amplification reactions are mainly divided into polymerase chain reactions, rolling loop replication amplification reactions, polymerase chain replacement reactions, hybridization chain reactions, and chain substitution reactions. Target cyclic amplification reactions can not only analyse and detect DNA sequences but also realize cyclic amplification of the detection signals of targets without enzymes, which greatly improves the detection sensitivity of targets [21-24].

In this work, we presented a highly sensitive electrochemical miRNA sensor based on pDNA/AuNPs/PMB/GCE coupled with a target cyclic signal amplification strategy (Scheme 1). The change in DPV response of a PMB film ( $\Delta I$ ) originating from miRNA/DNA hybridization on the surface of pDNA/AuNPs/PMB/GCE was adopted as a signal to detect target miRNA. In the presence of one copy of target miRNA, the target cyclic amplification reaction could be started, numerous H2 molecules were immobilized onto the electrode surface, and the structure of pDNA was destroyed, which resulted in an amplified signal and improved the detection sensitivity. MiRNA-21 was employed as a model to verify this strategy. Tests indicated that the proposed sensor demonstrated good selectivity and high sensitivity. Thus, the as-prepared sensor may have great potential in cancer diagnosis.



**Scheme 1.** Schematic representation showing the fabrication of the sensor and the detection of miRNA-21.

## 2. EXPERIMENTAL

### 2.1 Instruments and Reagents

Methylene blue, trisodium citrate, and sodium hydroxide were purchased from Sinopharm Group Chemical Reagent Co., Ltd. Alumina and potassium dihydrogen were purchased from Xilong Scientific Co., Ltd. Gold chloride acid was purchased from Alfa Aesar (Tianjing, China). The various sequences of DNA and RNA were synthesized by Shanghai Sangon Bioengineering (Shanghai, China) (Table 1). PBS solution (pH 7.0) was used to prepare stock solutions of DNA and RNA and stored in a freezer. Furthermore, 0.01 M PBS (0.1 M NaCl, 0.01 M PBS, pH 7.0) and 0.1 M PBS (pH 7.0) solutions were prepared. All chemicals used in this work were analytical reagent and used without further purification. All solutions were prepared with double-distilled water.

**Table 1.** DNA and RNA sequences

Sequence	5' - 3'
H1	ATAAGCTATCTACACATGGTAGCTTATCAGACTCCATGTGT AGA - (CH <sub>2</sub> ) <sub>6</sub> -SH
H2	TCAACATCAGTCTGATAAGCTACCATGTGTAGATAGCTTAT CAGACTCCTAATGGTGTGGC
miRNA-21	UAGCUUAUCAGACUGAUGUUGA
Two-base mismatched RNA	UAGGUUAUCAGACUGAUGGUGA

TEM measurements were carried out on a JEOL-2100 instrument with an acceleration voltage of 200 kV. Zeta potentials were measured on a Nano-Z Zetasizer. CV and DPV were operated on a CHI660A electrochemical workstation (Shanghai Chenhua Instruments, China). A three-electrode system (bare GCE or modified electrode: working electrode; saturated calomel electrode (SCE): reference electrode; platinum wire: counter electrode) was utilized. All electrochemical measurements were performed in the absence of oxygen, which was removed with high-purity N<sub>2</sub> for 15 min, and a blanket of N<sub>2</sub> was maintained over the solution during the measurements.

### 2.2 Preparation of AuNPs

AuNPs were synthesized according to a previous report [15]. Briefly, trisodium citrate (38.8 mM) was prepared, and then 30 mL was added to 1% HAuCl<sub>4</sub> solution under vigorous stirring. It was heated for 15 min and then allowed to cool to room temperature. The colour of the solution changed from light yellow to dark red, and it was finally stored at 4 °C until use.

### 2.3 Preparation of pDNA/AuNPs/PMB/GCE

The bare GCE was polished into a mirror-like finish with wet 1.0, 0.3, and 0.05  $\mu\text{m}$   $\text{Al}_2\text{O}_3$  powder and then ultrasonically washed with water and then anhydrous ethanol for 1 min each. After that, the treated GCE was immersed into 0.01 M PBS containing 2 mM MB. A continuous cyclic voltammetry scan was carried out in a potential range of -0.8 - +0.8 V at a scan rate of 100 mV/s for 20 cycles. The obtained electrode was named PMB/GCE. Twenty microliters of the as-synthesized AuNP solution was dropped onto the surface of the PMB/GCE for 12 h in a humid environment and then washed with distilled water three times. AuNPs could be immobilized onto the PMB film surface via electrostatic interactions. Thus, the AuNPs/PMB/GCE was prepared.

After that, the AuNPs/PMB/GCE was immersed in a 1.0  $\mu\text{M}$  H1 solution and kept at room temperature for 12 h, and the probe capture interface was formed on the surface of the electrode via Au-S binding. The obtained electrode was named pDNA/AuNPs/PMB/GCE.

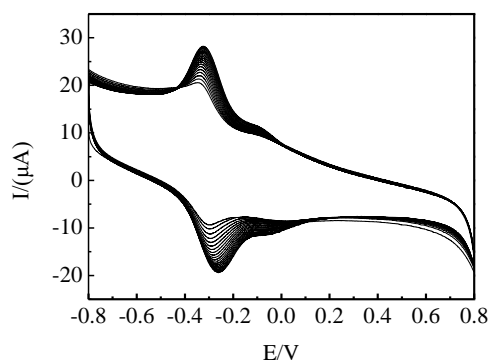
### 2.4 Detection of miRNA-21

pDNA/AuNPs/PMB/GCE was incubated with miRNA-21 in the presence of H2 (0.1  $\mu\text{M}$ ) at 37  $^\circ\text{C}$  for 90 min. The DPV signals were recorded by a CHI660A electrochemical workstation. The concentration of the target miRNA was quantified by the DPV reduction peak current change ( $\Delta I$ ) of the PMB film ( $\Delta I = I_{\text{ssDNA}} - I_{\text{dsDNA}}$ ).

## 3. RESULTS AND DISCUSSION

### 3.1 Continuous CV of MB

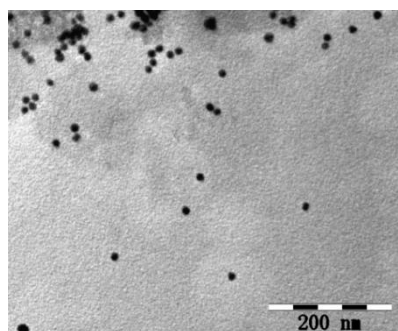
CV was used to fabricate a PMB film on the surface of the electrode, and the results are shown in Fig. 1. A pair of peaks appeared in the first cycle, which was attributed to the redox peaks of MB[25]. Then, the redox peak current of MB gradually increased with increased cycling, thus reflecting the continuous growth of the PMB film. When the scan reached 20 cycles, the peak current of MB barely increases, indicating that the polymerization reaction was complete. The above observation showed that the PMB film was successfully deposited on the GCE surface.



**Figure 1.** Continuous CV of MB on the bare GCE after an electro-initiated polymerization in 0.01 M PBS. Scan rate: 100 mV/s, MB: 2.0 mM, pH=7.0.

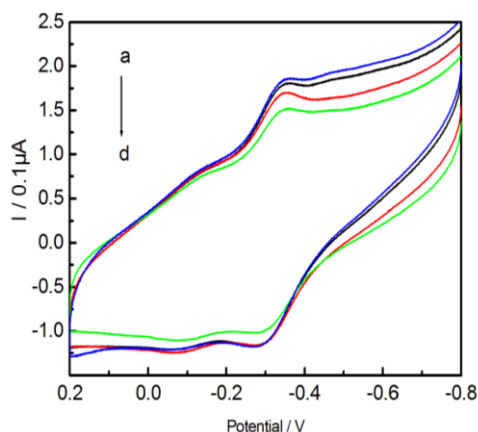
### 3.2 TEM of AuNPs

TEM was used to characterize the AuNPs. TEM images of AuNPs are shown in Fig. 2. The obtained nanoparticles were highly uniform and monodispersed, and the AuNP diameters were  $\approx 13$  nm. The zeta potential measurements showed that the AuNPs were negatively charged ( $\approx -23$ ), which was similar to a previous report [26].



**Figure 2.** TEM images of the AuNPs.

### 3.3 Feasibility of the proposed strategy



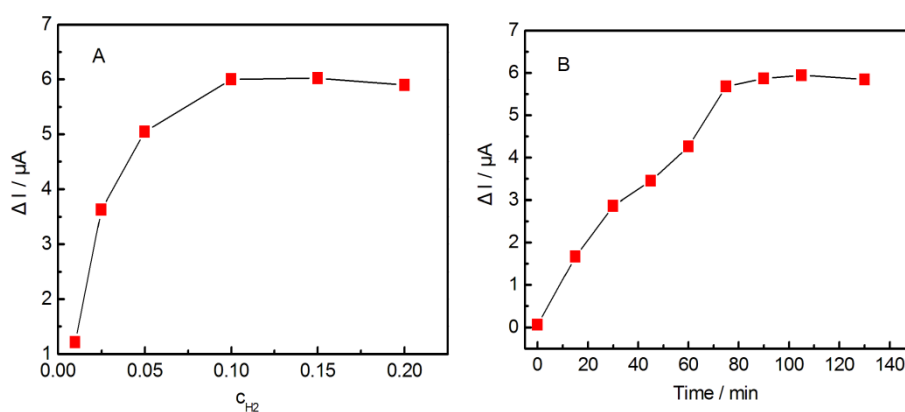
**Figure 3.** (A) CV curves of different electrodes in 0.1 M PBS at a scan rate of 100 mV/s: AuNPs/PMB/GCE (a), pDNA/AuNPs/PMB/GCE (b), and (b) incubated with miRNA-21 (c) or miRNA-21+H2 (d). Concentration of miRNA-21: 0.1  $\mu$ M.

Fig. 3 shows the CV curves of different electrodes in 0.1 M PBS: AuNPs/PMB/GCE (a), pDNA/AuNPs/PMB/GCE (b), and (b) incubated with miRNA-21 (c) or miRNA-21+H2 (d). The results revealed that the immobilization of pDNA led to a decrease in peak currents. After hybridization with target miRNA-21, the peak currents further decreased, which was similar to previous reports [27, 28]. These results indicated that the proposed strategy was reasonable and could be used to detect miRNA based on the change in the DPV peak current of the PMB film before and after target recognition. To verify the signal amplification of the proposed strategy, 0.1  $\mu$ M H2 was selected as the DNA fuel to start

the cycling amplification reaction, and the detection signal could be obviously improved in the presence of H<sub>2</sub>. In addition, only H<sub>2</sub> had no effect on the CV response of the PMB film, which indicated that the cycling amplification reaction could occur on the surface of the electrode. These results indicated that the proposed strategy was feasible.

### 3.4 Sensitivity and selectivity of the sensor

The concentration of H<sub>2</sub> and the incubation time of pDNA/AuNPs/PMB/GCE with miRNA-21 were optimized. The results are shown in Fig. 4. The optimum concentration of H<sub>2</sub> and incubation time were 0.1  $\mu$ M and 90 min, respectively.



**Figure 4.**  $\Delta I$  vs. the concentration of H<sub>2</sub> (A) and the incubation time (B).

Under the optimal experimental conditions, the proposed sensor was applied to measure different concentrations of miRNA-21 and various kinds of RNAs to verify its sensitivity and selectivity. As shown in Fig. 5, the DPV response of the PMB film gradually decreased after this sensor was incubated with different concentrations of miRNA-21.  $\Delta I$  was linear with the logarithm of the miRNA-21 concentrations in a range from  $1.0 \times 10^{-13}$ - $1.0 \times 10^{-9}$  mol/L, and the linear regression equation was  $\Delta I = 22.22 + 1.69 \lg c$  ( $R^2 = 0.98$ ); additionally, the detection limit was  $3.0 \times 10^{-14}$  mol/L ( $S/N=3$ ) (Fig. 5. inset). The linear range and detection limit of the proposed method were compared with published articles, as shown in Table 2 [28-30]. The comparison indicated that the proposed method performed well as an miRNA assay. Next, recovery experiments were conducted, and the recoveries were measured by the ratio between the found amount and the added amount. As shown in Table 3, the recoveries for miRNA-21 were 95%-102%. indicating that the established sensor was able to effectively detect miRNA in the samples.

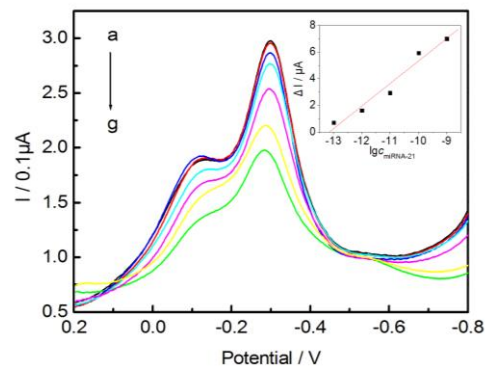


**Figure 5.** DPV of this sensor after incubation with different concentrations of miRNA-21: sensor (a); 0 (b);  $1.0 \times 10^{-13}$  M (c);  $1.0 \times 10^{-12}$  M (d);  $1.0 \times 10^{-11}$  M (e);  $1.0 \times 10^{-10}$  M (f);  $1.0 \times 10^{-9}$  M (g). Inset:  $\Delta I$  vs. the logarithm of the miRNA-21 concentrations.

**Table 2.** Comparison of the linear range and detection limit with similar sensors

Modified electrodes	Linear range (mol/L)	Detection limit (mol/L)	Ref.
AuNPs/GCE	$1.0 \times 10^{-12} \sim 1.0 \times 10^{-8}$	$3.0 \times 10^{-13}$	[28]
PNA/poly(JUG-co-JUGA)/GCE	$1.0 \times 10^{-8} \sim 1.0 \times 10^{-7}$	$1.0 \times 10^{-8}$	[29]
ssDNA/PICA/GCE	$3.34 \times 10^{-9} \sim 1.06 \times 10^{-8}$	$1.0 \times 10^{-9}$	[30]
AuNPs/PMB/GCE	$1.0 \times 10^{-13} \sim 1.0 \times 10^{-9}$	$3.0 \times 10^{-14}$	This paper

**Table 3.** Recovery experiment results for detecting miRNA-21

Sample no.	Added (mol/L)	Found (mol/L)	Recovery (%)
1	$1.0 \times 10^{-12}$	$9.50 \times 10^{-13}$	95.00
2	$1.0 \times 10^{-11}$	$9.82 \times 10^{-12}$	98.20
3	$1.0 \times 10^{-10}$	$1.02 \times 10^{-10}$	102.00

The selectivity of this sensor was studied by measuring  $\Delta I$  after incubating with various miRNAs. Fig. 6 shows the CV curves of the sensor incubated with the miRNA-21 target and mismatched RNA (the target miRNA-21 and two-base mismatched RNA concentrations were  $1.0 \times 10^{-9}$  mol/L). No signal change was observed for the blank solution or the two-base mismatched RNA. Importantly, an obvious increase in  $\Delta I$  was found for miRNA-21, indicating that the proposed sensor could distinguish various miRNA target sequences.

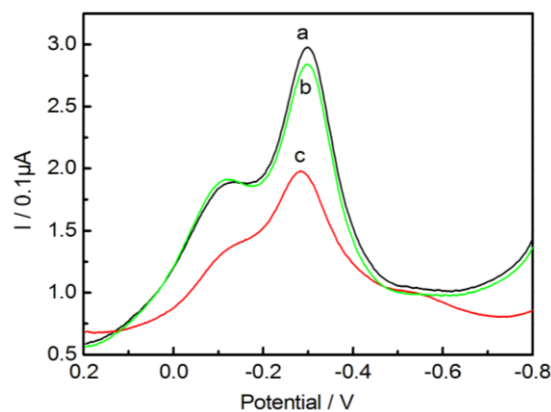


**Figure 6.** (A) DPV curves of the sensor incubated with various RNA samples: blank (a), two-base mismatched RNA (b), and miRNA-21 (c). The concentration of the miRNA samples was 1.0 nM.

#### 2.4 Reproducibility and stability

Three sensors were independently prepared and used to detect  $1 \times 10^{-9}$  mol/L miRNA-21 three times in parallel (R.S.D.=2.45%), which indicated that the sensor demonstrated excellent reproducibility. The same sensor was placed at room temperature for 4 d in PBS. The same concentration of miRNA-21 was detected three times in parallel, and no significant change in response signal was found, indicating that the sensor demonstrated good stability.

## 4. CONCLUSIONS

In this work, a sensitive electrochemical miRNA sensor, based on a AuNPs@PMB-modified electrode and target cyclic amplification strategy, was designed and employed to detect miRNA-21. The test results indicated that the sensor demonstrated high selectivity, good sensitivity, reproducibility, and stability. Thus, the as-prepared sensor has good application prospects for the analysis and detection of miRNA.

#### ACKNOWLEDGEMENTS

This work is supported financially by the Program of Study for Outstanding Young Scholar sponsored in Universities by Education Department of Anhui Province (gxgnfx2019051) 、 Open fund project of national and local joint engineering laboratory for crop stress resistance breeding and disaster reduction (NELCOF20190108) and Suzhou science and technology plan projects (Key technology and industrialization of improving valine fermentation level by atmospheric pressure room temperature plasma mutation breeding).

#### References

1. L. He, J. M. Thomson, M. T. Hemann, E. Hernando-Monge, D. Mu, S. Goodson, S. Powers, C. Cordon-Cardo, S. W. Lowe, G. J. Hannon, S. M. Hammond, *Nature*, 435(2005)828.



2. C. P. Liang, P. Q. Ma, H. Liu, X. G. Guo, B. C. Yin, B. C. Ye, *Angew. Chem. Int. Ed.*, 56(2017)9077.
3. X. W. Deng, Z. X. Yin, J. Q. Lu, X. L. Li, L. H. Shao, C. Y. Zhao, Y. S. Yang, Q. Hu, Y. Wu, W. Sheng, *Adv. Sci.*, 5(2018)1700542.
4. M. Lagos-Quintana, R. Rauhut, W. Lendeckel, T. Tuschl, *Science*, 294(2001)853.
5. J. T. Liu, P. Du, J. Zhang, H. Shen, J. P. Lei, *Chem. Commun.*, 54(2018)2550.
6. H. M. Ying, Z. Wu, B. Tu, W. H. Tan, J. H. Jiang, *J. Am. Chem. Soc.*, 139(2017)9779.
7. J. T. Yi, T. T. Chen, J. Huo, X. Chu, *Anal. Chem.*, 89(2017)12351.
8. L. M. Yang, B. Liu, M. M. Wang, J. Li, W. Pan, X. N. Gao, N. Li, B. Tang, *ACS Appl. Mater. Interfaces*, 10(2018)6982.
9. C. C. Pritchard, H. H. Cheng, M. Tewari, *Nat. Rev. Gene.*, 13(2012)358.
10. T. H. Seefel, W. J. Zhou, R. M. Corn, *Langmuir*, 27(2011)6534.
11. T. Yang, M. J. Chen, Q. Q. Kong, X. L. Luo, K. Jiao, *Biosens. Bioelectron.*, 89(2017)538.
12. M. Chen, C. J. Hou, D. Q. Huo, H. B. Fa, Y. N. Zhao, C. H. Shen, *Sens. Actuators, B*, 239(2017)421.
13. S. Su, H. F. Sun, W. F. Cao, J. Chao, H. Z. Peng, X. L. Zuo, L. H. Yuwen, C. H. Fan, L. H. Wang, *ACS Appl. Mater. Interfaces*, 8(2016)6826.
14. K.Y. Zhang, N. Zhang, L. Zhang, H.Y. Wang, H.W. Shi, Q. Liu, *RSC Adv.*, 8(2018)16146.
15. S. Yu, Y.Y. Wang, L.P. Jiang, S. Bi, J.J. Zhu, *Anal. Chem.*, 90(2018)4544.
16. X.M. Guo, Z.H. Wang, J.F. Xia, *Acta Anal. Sinica*, 31(2012)464.
17. D.B. Gorle, M. A. Kulandainathan, *RSC Adv.*, 6(2016) 19982.
18. J. Shan, L.Y. Wang, Z.F. Ma, *Sens. Actuators B: Chemical*, 237(2016) 666.
19. Q. Wang, Q. Li, X.H. Yang, K.M. Wang, S.S. Du, H. Zhang, Y.J. Nie, *Biosens. Bioelectron.*, 77(2016)1001.
20. L. Tian, K. Qian, J.X. Qi, Q.Y. Liu, C. Yao, W. Song, Y.H. Wang, *Biosens. Bioelectron.*, 99(2018)564.
21. S. Bi, S. Z. Yue, S. S. Zhang, *Chem. Soc. Rev.*, 46(2017)4281.
22. K. W. Ren, Y. F. Xu, Y. Liu, M. Yang, H. X. Ju, *ACS Nano*, 12(2018)263.
23. L. He, D. Q. Lu, H. Liang, S. T. Xie, X. B. Zhang, Q. L. Liu, Q. Yuan, W. H. Tan, *J. Am. Chem. Soc.*, 140(2018) 258.
24. Q. S. Guo, F. K. Bian, Y. Q. Liu, X. J. Qu, X. Y. Hu, Q. J. Sun, *Chem. Commun.*, 53(2017)4954.
25. M.B. Gholivand, E. Ahmadi, M. Haseli, *Anal. Biochem.*, 527(2017)4.
26. K.Y. Zhang, S.T. Song, S. Huang, L. Yang, X.C. Wu, F. Lu, J.J. Zhu, *Small*, 14(2018)1802292.
27. K.Y. Zhang, Yuzhong Zhang, *Electroanalysis*, 22(2010)673.
28. D. Zhu, W. Liu, D.X. Zhao, Q. Hao, J. Li, J.X. Huang, J.Y. Shi, J. Chao, S. Su, L. H. Wang, *ACS Appl. Mater. Interfaces*, 9(2017)35597.
29. 27N. P. Pu, P. zhang, Y. Zhuo, *Chem. Sens.*, 36(2016)48.
30. 28S. Reisberg, L. A. Dang, Q. A. Nguyen, B. Piro, V. Noel, P. E. Nielsen, L. A. Le, M. C. Pham, *Talanta*, 76(2008)206.
31. 29X. M. Li, J. P. Xia, S. S. Zhang, *Anal. Chim. Acta*, 622(2008)104.